Accumulation of brain hypointense foci on susceptibility-weighted imaging in childhood ataxia telangiectasia

Rob A Dineen, PhD[1,2,3], Caroline C V Blanchard, PhD[1], Stefan Pszczolkowski, PhD[1], Simon Paine, PhD[4], Manish Prasad, MD[5], Gabriel Chow, MD[5], William P Whitehouse, FRCPCH[5,6], Dorothee P Auer, PhD[1,2,3]

Author Affiliations:

1 Radiological Sciences, Division of Clinical Neuroscience, University of Nottingham

2 Sir Peter Mansfield Imaging Centre, University of Nottingham

3 NIHR Nottingham Biomedical Research Centre

4 Department of Pathology, Nottingham University Hospitals NHS Trust

5 Nottingham Children's Hospital, Nottingham University Hospitals NHS Trust

6 Division of Child Health, University of Nottingham

Grant Support:

The funding for the research was from research grants awarded jointly by A-T Children's Project and Action for A-T [grant ref: 'The CATNAP Study'], and jointly by Action for A-T and BraShA-T [grant ref: 17NOT03]. The funders had no role in the study design; the collection, analysis and interpretation of data; the writing of the report; and the decision to submit the article for publication.

Corresponding Author:

Dr Rob A Dineen.

Postal Address: Room A39i, Medical School, Queen's Medical Centre, Derby Road, Nottingham, NG7 2UH, United Kingdom.

Phone: 0115 8231173

Email: rob.dineen@nottingham.ac.uk

Abstract

Background and Purpose

Susceptibility-weighted imaging (SWI) hypointense cerebral lesions have been reported in adults with the inherited cerebellar neurodegenerative disorder ataxia telangiectasia (A-T). This study aims to establish the prevalence, age-dependency and spatial distribution of these lesions in children and young people with A-T.

Materials and Methods

Participants with classic A-T and matched controls underwent SWI acquisition at 3T at one or two time-points. SWI hypointense lesions were manually labelled according to the Microbleed Anatomical Rating Scale. Differences in prevalence of lesion number between A-T and non-A-T groups was tested with Fisher's exact test, and differences in age between A-T participants with and without lesions were tested using independent samples Mann-Whitney U. The relationship between age and lesion number was modelled as an exponential function.

Results

Analysable SWI datasets from 17 participants with A-T (median age 12.4 [range 4.6-20.2] years; 47% female) and 22 matched healthy controls showed prevalence of

SWI hypointense lesions in 41% of A-T participants and 0% in controls (p=0.001, *Fisher's exact test*). Lesions were exclusively supratentorial and predominantly lobar. A-T participants with SWI hypointense lesions were older than those without (median 15.2 years versus 9.3 years, *U*=10.5, p=0.014). An exponential curve described the relationship between age and lesion number (R^2 = 0.67).

Conclusion

SWI hypointense lesions are common in children and young people with A-T, accumulating from 12 years onwards. In contrast to cerebellar-dominant neurodegeneration in A-T, SWI hypointense lesions were exclusively supratentorial. Further investigation is needed to establish the clinical relevance of these imaging-detected lesions.

Introduction

Ataxia Telangiectasia (A-T, OMIM #208900) is an autosomal recessive multisystem disorder associated with cerebellar neurodegeneration, telangiectasia (particularly conjunctival), immunodeficiency, pulmonary disease, radiation sensitivity and cancer predisposition[1]. People with 'classical' A-T have either no production of the ATM protein or produce ATM protein which is completely non-functioning. People who produce a significantly reduced amount of functioning ATM have milder 'variant' A-T[2].

Cerebellar atrophy is the dominant neuroimaging finding in A-T (reviewed in detail by Sahama and colleagues[3]), but several case series and individual case reports describe hypointense foci in the brain parenchyma using susceptibility-weighted imaging (SWI) or T2*-weighted imaging. In a series of 10 adults with A-T aged 19-34 years, Lin *et al* observed hypointense foci using SWI in 7 (70%) of the participants[4]. These ranged from a single hypointense focus in a 21-year old through to 'innumerable' foci in individuals aged 28 and 34 years. Wallis and colleagues presented a series of 12 adults with A-T aged 23–47 years, 4 of whom had hypointense foci (solitary in 2, multiple in 2) in the brain parenchyma on T2*-weighted imaging[5]. Further examples are provided by Liu and colleagues[6] (27-year-old man with multiple hypointense foci on SWI) and Ciemins and Horowitz[7] (31-year-old female with multiple hypointense foci on both T1- and T2-weighted images).

To date the prevalence, age distribution and spatial distribution of SWI hypointense foci in the brains of children with A-T has not been investigated. To address this we use data from the Childhood A-T Neuroimaging Assessment Project (CATNAP)[8] to

test the hypothesis that SWI hypointensities accumulate during childhood in children and young people with classical A-T.

Materials and Methods

The data for this analysis are from the first and second phases CATNAP. In brief, the first phase of CATNAP involved the acquisition of multi-parametric MRI and neurological data from children and young people aged 6 to 18 years with A-T and matched healthy controls. As described previously[8], participants with A-T were recruited from the UK National Paediatric A-T Clinic and were excluded if they had contra-indication to MRI, concurrent or previous cancer or cancer treatment, or other (non-A-T) neurological or neurosurgical condition. Healthy volunteers were recruited from local community groups, and excluded if they had contra-indication to MRI or any neurological, neurosurgical or other significant medical condition. Recruitment ran from January 2015 to September 2016. The results of volumetric analysis and spectroscopy have been reported[8]. The second phase of CATNAP involved invitation of previous participants for repeat multi-parametric MRI on the same scanner using an identical protocol after an interval of 2-4 years, and recruitment of new participants aged 3-6 years to test the feasibility of the data acquisition in very young children. Informed consent was obtained from participants aged 16 to 18 years and from parents / guardians of participants aged under 16 years. The first and second phases of CATNAP were approved by UK National Research Ethics Service (references 14/EM/1175 and 18/SW/0078 respectively).

Image Acquisition and Analysis

All participants underwent MRI scanning on 3T Discovery MR750 (GE Healthcare, Milwaukee, WI) with 32-channel head coil, without sedation. In addition to standard paediatric MRI preparation, younger participants were shown an animation to prepare them for MRI[9] and were able to watch video content during the scan on an MRI compatible monitor. The full MRI protocol is detailed in the supplementary materials. The results presented here relate to the axial SWI acquisition performed using the SWAN (T2 Star Weighted ANgiography) susceptibility-based 3D multi-echo gradient sequence (216 slices, slice thickness 1mm with 0.5 mm between slices, FOV = 256 x 256, TR= 39.3ms, effective TE= 24.68ms, flip angle=15, scan duration 4:19).

Two experienced neuroradiologists (R.A.D., D.P.A) who were unaware of disease status independently labelled all hypointensities manually on SWI according to the anatomical classification specified in the microbleed anatomical rating scale (MARS)[10] using the paintbrush drawing tool in ITK-SNAP software (http://www.itksnap.org)[11]. Following the independent review, any discrepancies in lesion labelling were resolved through discussion leading to consensus.

Statistical Analysis

*C*omparison of age distribution between the A-T and non-A-T groups was performed using the independent samples Mann-Whitney U test. Prevalence of SWI hypointense lesions (using second scan for those with two scans) was expressed as a percentage with 95% confidence intervals (95%CI) for each group, and differences in prevalence of SWI hypointense lesions between A-T and non-A-T groups was

tested using Fisher's exact test. Within the A-T group, differences in age distribution between those with and without SWI hypointense lesions was performed using the independent samples Mann-Whitney U test, using age at second scan for those with two scans. Exact significance (two-tailed) was calculated and significance level was set at $\alpha < 0.05$. We modelled the relationship between age and observed number of SWI hypointense lesions as an exponential function $y = a \cdot e^{b \cdot x}$, where x is age, y is the observed number of lesions, and a and b are unknown parameters. In order to find the values of a and b that best fitted the data, we ran a Trust Region Reflective optimisation[12, 13] with a starting point of $a = 0.01,\ b = 0.5$.

Results

Twenty-two children and young people with A-T and twenty-two without A-T underwent at least one SWI acquisition. Of these, 8 with A-T and 13 without A-T had a second SWI scan. In total, 13 of the SWI datasets (10 from the A-T group and 3 from the non-A-T group) were excluded from the analysis due to significant participant motion artefacts. One scan where the image quality was felt to be borderline showed a clear parenchymal SWI hypointense lesion and this scan was retained in the analysis. The analysed images were from 17 children and young people with A-T (median age at first scan 12.4 [range 4.6-20.2] years; 8 (47%) female) and 22 without-A-T (median age at first scan 13.0 [range 5.5-17.8] years; 11 (50%) female). No group difference in age distribution (U = 188, exact p = 0.977). Analysable second SWI scans were available from 2 people in the A-T group (interscan intervals of 3.3 and 3.5 years) and from 10 in the non-A-T group (median interscan interval 2.4 years, range 2.3-3.5 years). Of the17 participants with A-T

included in this report, 8 had no ATM expression, 8 had ATM expression but no kinase activity and 1 had ATM expression with some residual kinase. No participant with A-T reported (or had parental / carer report of) an alternative cause for cerebral microbleeds, such as history of head trauma, hypertension or coagulopathy. Sixteen of the participants with A-T and 21 of the participants without A-T were included in our previous publication relating to cerebellar volumetry, diffusion and spectroscopy[8]. Recruitment to CATNAP and CATNAP-2 and the availability of acceptable-quality SWI data is summarised in the flowchart (supplementary figure 1).

SWI hypointense lesions were present in 7 out of 17 participants with A-T on at least one scan, giving a prevalence of 41% (95%CI 22-64%) (Figure 1). For the 7 participants with A-T who had SWI hypointense lesions, the number of lesions ranged from 1 to 41 (median = 3) (Figure 2). Lesions ranged in size from 2mm (the lower limit for inclusion[10]) up to 4mm. No lesions were identified in any participants in the non-A-T group, 0/22 (95%CI 0-18%). The prevalence of lesions differed significantly between the A-T and non-A-T groups (p=0.001, *Fisher's exact test*). Anatomical distribution of SWI hypointense lesions in the A-T group is shown in Table 1 and Figure 3. No SWI hypointense lesions were found in the cerebellum and brainstem, and supratentorial lesions were overwhelmingly lobar rather than deep. The SWI hypointense lesions were not clearly visible on the T1-weighted FSPGR images (Figure 1, bottom row).

A significant age difference was identified between A-T participants who did and did not have SWI hypointense lesions (median age 15.2 [range 12.4-20.2] years versus

9.3 [range 4.6-17.6] years respectively, *U* = 10.5, p = 0.014; Figure 4). No lesions were identified in children with A-T below the age of 12 years. The two participants with A-T who had analysable scans at two time-points both showed an increase in the number of lesions between the first and second scans (Figures 2 and 5). The curve fitted for the number of SWI hypointense lesions against age for the A-T group (Figure 2) had $R^2 = 0.67$ and was described by the equation:

$$\text{number of lesions} = 0.00168 \cdot e^{0.4841 \cdot \text{age}}.$$

The 95% confidence limits for coefficient a are -0.00917 and 0.01252, and for coefficient b are 0.1575 and 0.8106.

Discussion

In our cohort of children and young people with A-T we identified a prevalence of SWI hypointense lesions of 41%. In comparison, no such lesions were identified in any participants of the well matched control group. Furthermore, despite the limited number of data points in the A-T group, we demonstrate a clear relationship between the number of SWI hypointense lesions and age across the group, as well as direct evidence on new lesion accumulation in the two A-T participants who had analysable SWI at two time points.

Previous case reports and series have reported SWI hypointense lesions in adults with A-T, but the prevalence and natural history of these lesions in children with A-T was not known. Indeed, Lin and colleagues state that in their clinical experience SWI hypointense lesions are absent in children with A-T, and that lesions are

acquired and only cross a threshold of detectability in early adulthood[4]. Our findings support the notion that lesions are acquired in an age-related manner, but counter the statement relating to absence in childhood. It is possible that improvements in acquisition of SWI images since the time of that publication in 2014 allow us to visualise lesions more clearly.

The nature and significance of these imaging-detected lesions remains uncertain. Histopathological studies have demonstrated the presence of a distinctive vascular abnormality in people with A-T referred to as 'gliovascular nodules'[14]. These consist of dilated capillary loops, often containing fibrin thrombi, around which there is perivascular haemorrhage and haemosiderin deposition with associated demyelination and astrocytic gliosis, including atypical forms, some of which contain eosinophilic cytoplasmic inclusions, in the adjacent parenchyma[15, 16]. It is likely that the focal hypointensities detected in our work and by previous studies are the *in-vivo* imaging correlate of these gliovascular nodules, although direct correlation between imaging and histopathology has not been performed to our knowledge. Notably, pathological studies show that the distribution of gliovascular nodules is predominantly in the cerebral white matter, occasionally in the basal ganglia and cerebral cortex, but not in the cerebellum. This description of location matches closely the distribution of lesions found in our data. The reason for the observed distribution of lesion is not known, nor why the posterior fossa appears to be spared. There may be underlying factors related to vascular structure and / or vascular expression of different molecules or receptors, or there may be a relationship to haemodynamic parameters. Combined imaging, histopathological and molecular

studies may help to clarify the underlying causes of the formation and distribution of the lesions.

However, it is also possible that pathological changes other than gliovascular nodules could account for the imaging appearances. An histopathological case report described hyalinisation of cerebral blood vessels associated with intimal and adventitial hypertrophy in a patient with advanced disease[17], indicating the presence of cerebrovascular degenerative pathology that is separate from the gliovascular nodules. However, the limited available reports do not suggest that this cerebrovascular hyalinsation occurring with A-T is directly associated with localised microhaemorrhage or haemosiderin deposition detected by SWI. Lin at al[4] comment that CNS irradiation can cause similar appearances on SWI due to the development of radiation-induced cavernous haemangiomas, which can be seen as a late sequelae of cancer treatment[18]. This may be relevant because A-T is associated with an increased cellular sensitivity to ionising radiation[19] and abnormal DNA damage response. However, the histopathological description of vascular changes seen in A-T do not closely overlap with those described for radiation-induced cavernous haemangiomas which appear to show two distinct histological patterns; those resembling typical cerebral cavernous haemangiomas and those caused by radiation-induced fibrinoid vascular necrosis and vascular leakage[20].

It is currently unclear whether the presence of the hypointense lesions on SWI in people with A-T confers an increased risk of intracerebral haemorrhage. In other conditions with similar appearing lesions on SWI, such as cerebral amyloid angiopathy and cerebral cavernous haemangiomas, the presence of lesions

indicates an increased macrohaemorrhage risk[21, 22]. There are only two reports of macrohaemorrhage in people with A-T[23, 24], but the relationship to any underlying SWI hypointensities has not been explored.

In other regards, the relationship between presence or number of SWI hypointense lesions and other clinical or imaging manifestations of A-T is also not known. Of particular interest is the question of whether SWI hypointense lesions could impact on cognitive function. Previous studies have identified cognitive deficits in people with A-T including in the domains of language, processing speed, visuospatial processing, working memory, attention and abstract reasoning[25, 26], which have been attributed to the cerebellar cognitive affective syndrome[27]. Given that other diseases associated with multifocal cerebral white matter lesions, such as multiple sclerosis[28] and small vessel disease[29], are associated with cognitive dysfunction, an impact of cerebral SWI hypointense lesions on cognition in people with A-T is possible. The small number of participants with A-T showing SWI hypointense lesions in our dataset limits further exploration of the relationship between the presence or number of these lesions and other neurological, cognitive or imaging metrics. Ideally future, larger imaging studies in A-T will include SWI acquisitions allowing the clinical relevance of these lesions to be formally investigated.

This study is the largest reported series of SWI in childhood A-T and has a well matched control group, but is still limited by small sample size. There was a high rate of data rejection in the A-T group (one third of the SWI datasets) due to excessive participant motion rendering the image unreliable for analysis, which

reduced the number of longitudinal SWI datasets in the A-T group from 8 to 2. We employed careful participant preparation and carefully immobilised the participant's head in the head coil using inflatable pads. However, A-T is a movement disorder and those affected are prone to involuntary movements. In addition, the SWI acquisition was towards the end of a multi-sequence research MRI protocol, which is likely to have affected tolerance and led to restlessness. We have taken steps to reduce observer bias during the identification of SWI hypointense lesions, which was performed independently by two experienced neuroradiologists who were not aware of the disease status. However, people with A-T typically have overt cerebellar atrophy that would have been visible on the SWI datasets during the labelling of SWI hypointense lesions and it is possible that the reviewing neuroradiologists may have unintentionally recognised that a scan was from a participant with A-T.

In summary, this work demonstrates that SWI hypointense lesions are present in children and young people with A-T with a prevalence of 41% and show accumulation across the childhood age range. No lesions were seen in children under 12 years. Furthermore, in our cohort lesions were exclusively supratentorial in an overwhelmingly lobar distribution, which is notable because the burden neurodegeneration in people with A-T occurs in the cerebellum[3]. Further investigation is needed to elucidate the nature and relevance of these imaging-detected lesions.

Acknowledgements

The authors would like to thank the children, young people and families who participated in the CATNAP studies. We also gratefully acknowledge the support Kay Atkins, Anne Murray

and William Davis and at the AT Society for support with publicising the study and arranging schedules and transport for participant visits; Dr Min Ong and Dr Ouliana Panagioti for additional support with neurological assessments; Mr Andrew Cooper for performing the MRI scans; Mrs Catherine Gibney for undertaking play preparation with younger participants; and Dr Felix Raschke, Ms Hannah McGlashan and Dr Jeyanthi Rangaraj for recruitment and additional participant assessments.

Funding

The funding for the research was from research grants awarded jointly by A-T Children's Project and Action for A-T [grant ref: 'The CATNAP Study'], and jointly by Action for A-T and BraShA-T [grant ref: 17NOT03]. The funders had no role in the study design; the collection, analysis and interpretation of data; the writing of the report; and the decision to submit the article for publication.

References

1. Rothblum-Oviatt C, Wright J, Lefton-Greif MA, et al. Ataxia telangiectasia: a review. *Orphanet J Rare Dis* 2016;11:159
2. Schon K, van Os NJH, Oscroft N, et al. Genotype, extrapyramidal features, and severity of variant ataxia-telangiectasia. *Ann Neurol* 2019;85:170-180
3. Sahama I, Sinclair K, Pannek K, et al. Radiological imaging in ataxia telangiectasia: a review. *Cerebellum* 2014;13:521-530
4. Lin DD, Barker PB, Lederman HM, et al. Cerebral abnormalities in adults with ataxia-telangiectasia. *AJNR Am J Neuroradiol* 2014;35:119-123
5. Wallis LI, Griffiths PD, Ritchie SJ, et al. Proton spectroscopy and imaging at 3T in ataxia-telangiectasia. *AJNR Am J Neuroradiol* 2007;28:79-83
6. Liu HS, Chen YC, Chen CY. Cerebral microbleeds and iron depletion of dentate nuclei in ataxia-telangiectasia. *Neurology* 2016;87:1062-1063
7. Ciemins JJ, Horowitz AL. Abnormal white matter signal in ataxia telangiectasia. *AJNR Am J Neuroradiol* 2000;21:1483-1485
8. Dineen RA, Raschke F, McGlashan HL, et al. Multiparametric cerebellar imaging and clinical phenotype in childhood ataxia telangiectasia. *Neuroimage Clin* 2020;25:102110
9. McGlashan HL, Dineen RA, Szeszak S, et al. Evaluation of an internet-based animated preparatory video for children undergoing non-sedated MRI. *Br J Radiol* 2018;91:20170719
10. Gregoire SM, Chaudhary UJ, Brown MM, et al. The Microbleed Anatomical Rating Scale (MARS): reliability of a tool to map brain microbleeds. *Neurology* 2009;73:1759-1766
11. Yushkevich PA, Piven J, Hazlett HC, et al. User-guided 3D active contour segmentation of anatomical structures: significantly improved efficiency and reliability. *Neuroimage* 2006;31:1116-1128
12. Branch MA, Coleman TF, Li Y. A Subspace, Interior, and Conjugate Gradient Method for Large-Scale Bound-Constrained Minimization Problems. *SIAM Journal on Scientific Computing* 1999;21:1-23
13. Coleman TF, Li Y. On the convergence of interior-reflective Newton methods for nonlinear minimization subject to bounds. *Mathematical Programming* 1994;67:189-224
14. Boder E. Ataxia Telangiectasia. In: Gomez MR, ed. *Neurocutaneous disorders*. Stoneham, MA: Butterworth Publishers; 1987:95-117
15. Amromin GD, Boder E, Teplitz R. Ataxia-telangiectasia with a 32 year survival. A clinicopathological report. *J Neuropathol Exp Neurol* 1979;38:621-643
16. Agamanolis DP, Greenstein JI. Ataxia-telangiectasia. Report of a case with Lewy bodies and vascular abnormalities within cerebral tissue. *J Neuropathol Exp Neurol* 1979;38:475-489
17. Kamiya M, Yamanouchi H, Yoshida T, et al. Ataxia telangiectasia with vascular abnormalities in the brain parenchyma: report of an autopsy case and literature review. *Pathol Int* 2001;51:271-276
18. Jain R, Robertson PL, Gandhi D, et al. Radiation-induced cavernomas of the brain. *AJNR Am J Neuroradiol* 2005;26:1158-1162
19. Huo YK, Wang Z, Hong JH, et al. Radiosensitivity of ataxia-telangiectasia, X-linked agammaglobulinemia, and related syndromes using a modified colony survival assay. *Cancer Res* 1994;54:2544-2547
20. Kleinschmidt-DeMasters BK, Lillehei KO. Radiation-Induced Cerebral Vascular "Malformations" at Biopsy. *J Neuropathol Exp Neurol* 2016;75:1081-1092
21. Charidimou A, Imaizumi T, Moulin S, et al. Brain hemorrhage recurrence, small vessel disease type, and cerebral microbleeds: A meta-analysis. *Neurology* 2017;89:820-829
22. Kearns KN, Chen CJ, Yagmurlu K, et al. Hemorrhage Risk of Untreated Isolated Cerebral Cavernous Malformations. *World Neurosurg* 2019;131:e557-e561

23. Casaril M, Gabrielli GB, Capra F, et al. [Ataxia telangiectasia. Description of a case with multiple cerebral hemorrhages and liver cirrhosis]. *Minerva Med* 1982;73:2183-2188
24. Nardelli E, Fincati E, Casaril M, et al. Multiple cerebral hemorrhages in ataxia-telangiectasia. A case report. *Acta Neurol (Napoli)* 1985;7:494-499
25. Hoche F, Frankenberg E, Rambow J, et al. Cognitive phenotype in ataxia-telangiectasia. *Pediatr Neurol* 2014;51:297-310
26. Vinck A, Verhagen MM, Gerven M, et al. Cognitive and speech-language performance in children with ataxia telangiectasia. *Dev Neurorehabil* 2011;14:315-322
27. Hoche F, Daly MP, Chutake YK, et al. The Cerebellar Cognitive Affective Syndrome in Ataxia-Telangiectasia. *Cerebellum* 2019;18:225-244
28. Dineen RA, Vilisaar J, Hlinka J, et al. Disconnection as a mechanism for cognitive dysfunction in multiple sclerosis. *Brain* 2009;132:239-249
29. Meng D, Hosseini AA, Simpson RJ, et al. Lesion Topography and Microscopic White Matter Tract Damage Contribute to Cognitive Impairment in Symptomatic Carotid Artery Disease. *Radiology* 2017;282:502-515

Tables

Table 1: Anatomical distribution of SWI hypointense lesions in the A-T Group.

	A-T (n=17)	
	Number of subjects with lesions	Total number of lesions
Lobar	6 (35%)	82
Deep grey matter	4 (24%)	7
Cerebellum	0 (0%)	0
Brainstem	0 (0%)	0
All sites	7 (41%)	89

Figures Legends

Figure 1 – Top row: Example of parenchymal SWI hypointense lesions in a participant with A-T aged 17.8 years. Axial images showing 4 separate lesions (white arrows). A total of 23 similar lesions (not all shown) were present on the imaged volume. Bottom row: Corresponding axial FSPGR images showing that the lesions are not clearly visible on the T1-weighted volumetric acquisition.

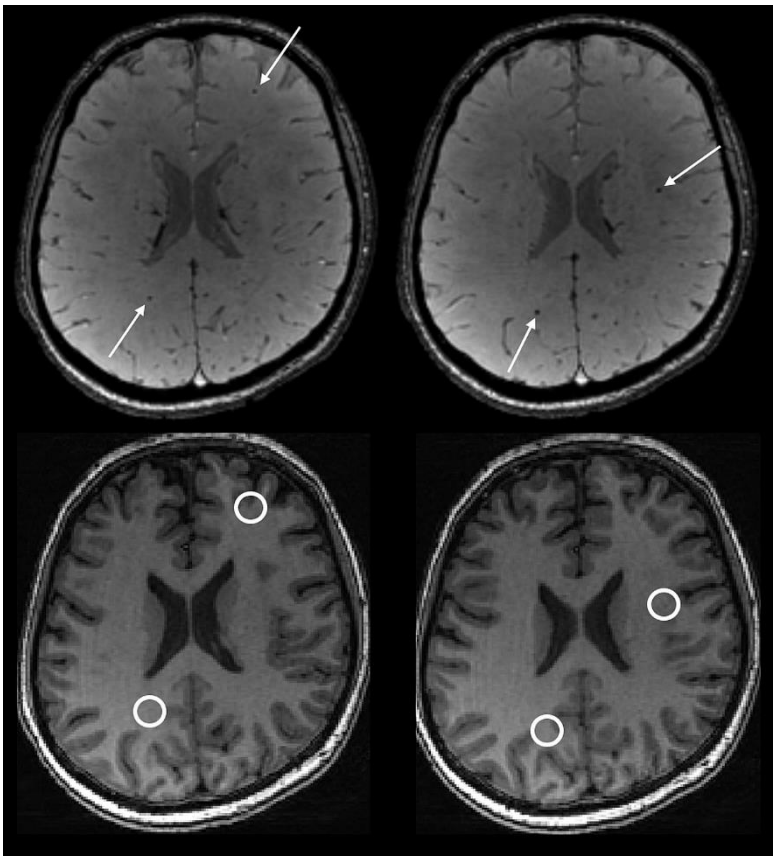

Figure 2 - Scatterplots showing relationship between age and number of lesions in people with A-T (top chart, blue) and people without A-T (bottom chart, green). Dotted lines indicate pairs of scans performed in the same individual. The curved blue line indicates the exponential model fitted to the data, with the blue shaded area indicating the 95% confidence intervals.

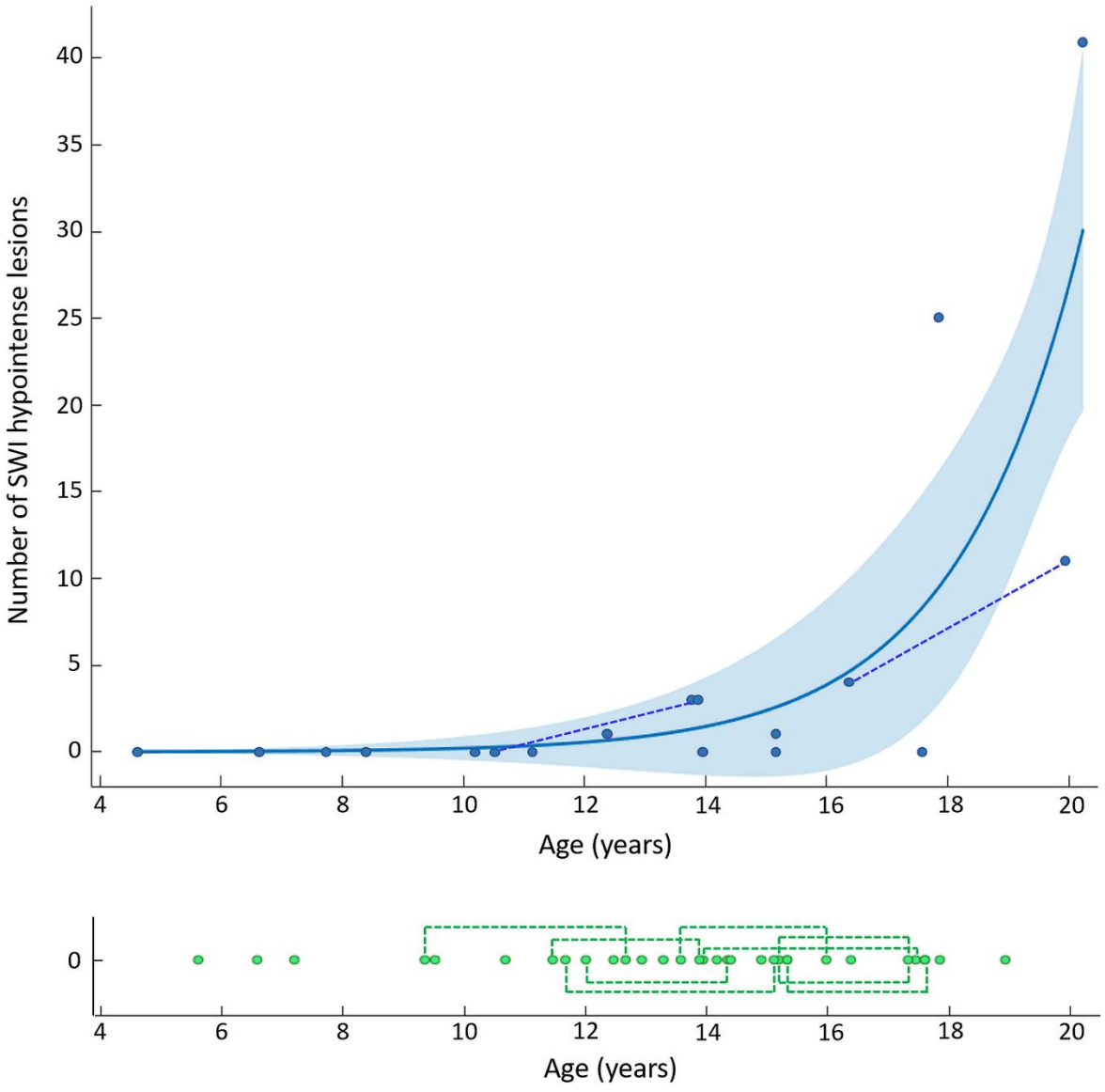

Figure 3 – Distribution of SWI hypointense lesions. Representative axial images from the summated SWI hypointense lesion maps from all participants with A-T, displayed on an MNI152 template. Axial slice locations indicated by the z-axis coordinate. Note the absence of cerebellar or brainstem lesions. Bottom right image: The same summated lesion map data displayed as a 3-D rendered image.

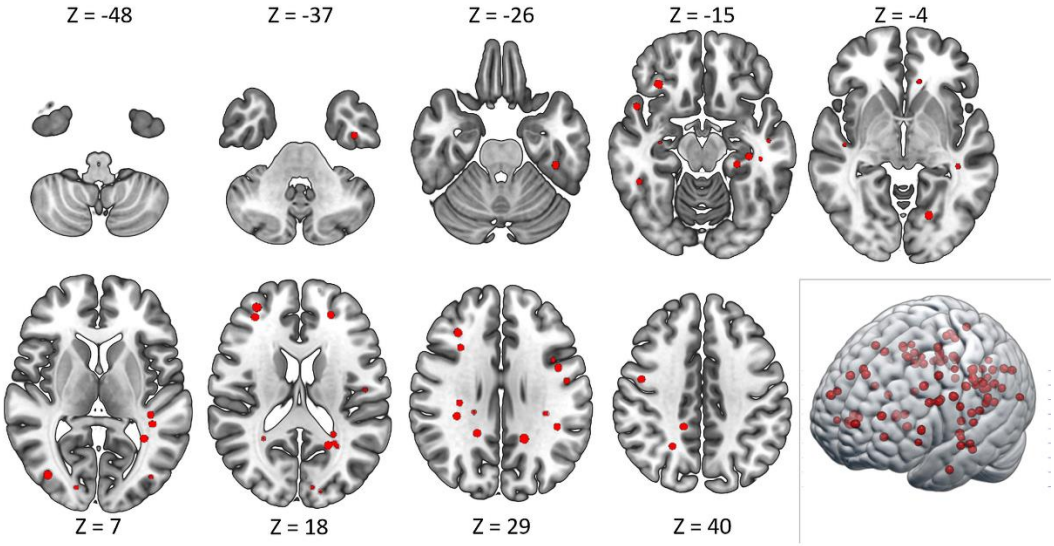

Figure 4 - Boxplot showing age distribution for A-T participants without (light grey) and with (dark grey) SWI hypointense lesions.

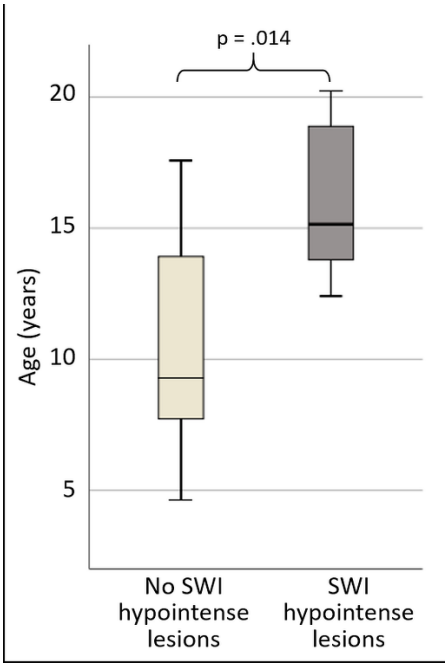

Figure 5 – Examples of new lesions in participants with A-T who had scans at two time points. Top and bottom rows indicate different participants; ages indicated on each image.

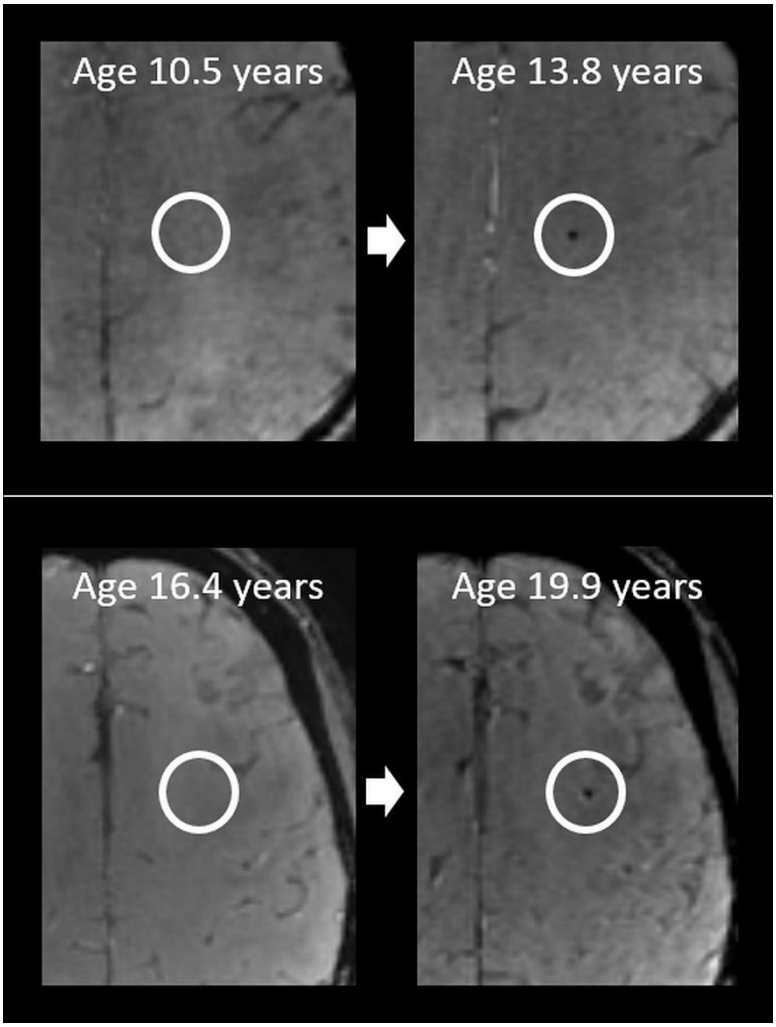

Supplementary materials

Full MRI Protocol for CATNAP and CATNAP2

MRI scanning was performed on 3T Discovery MR750 (GE Healthcare, Milwaukee, WI) with 32-channel head coil, without sedation. The multiparametric MRI scan protocol included:

- 3D fast spoiled gradient echo T1-weighted structural MRI (1mm isotropic resolution, TR=8.15ms, TE=3.172ms, TI=900ms, FOV=256x256x156mm);
- EPI-based axial diffusion-weighted imaging (participants were scanned with at least one of two sequences, a longer protocol for those tolerating the scan well: TR=8000ms, TE=63ms, b=1000s/mm2, 32 separate non-orthogonal directions, 4 additional b=0s/mm2 images acquired, 2mm isotropic voxel size, whole brain coverage, number of slices= 66; or shorter protocol if not tolerating the scan well: TR=8000ms, TE=83ms, b=1000s/mm2, 3 orthogonal directions, 0.9mm x 0.9mm x 4mm voxel size, number of averages = 2, whole brain coverage, number of slices= 30)
- Pulsed continuous arterial spin labelling (pCASL) with a 3D spiral read out (Flip angle 111^0, TR=4632ms, TE= 10.5ms, labelling duration 1450ms, post labelling duration=1525ms, FOV=240MM, slice thickness=4mm, slice gap=4mm, 36 axial slices, echo train length=1, number of excitations=3, matrix=128 x 128. Background suppression was used, and an M0 image collected for image quantification
- SWAN (T2* Weighted ANgiography) susceptibility-based 3D multi-echo gradient sequence (216 axial slices, slice thickness 1mm with 0.5 mm between slices, FOV = 256 x 256, TR= 39.3ms, effective TE= 24.68ms, flip angle=15). (Performed in a subset of participants)
- Neuromelanin-sensitive T1-weighted 3D spoiled gradient recalled (SPGR) images with magnetization transfer (TR: 38.4ms; TE: 3ms; Flip angle: 20; slice thickness: 2mm; FOV: 19.2; matrix: 480×192; scanning time: 3.25min. 30 axial slices). (Performed in a subset of participants)
- Resting-state functional MRI (TR: 2000ms; TE: 32 ms, FA: 90^0, matrix: 64 × 64, voxel size: 3.75 × 3.75 × 3.6 mm, 160 volumes. 35 axial slices). (Performed in a subset of participants)
- Single voxel MR spectroscopy with midline cerebellar voxel location16 (MEGA-PRESS with GSH editing, TR=2s, TE=131ms and 128 ON and 128 OFF acquisitions; voxel dimensions x=50mm y=22mm z=22mm; spectral editing using 20ms sinc-weighted Gaussian pulses at 7.5 ppm (OFF) and 4.54 ppm (ON)). (Performed in a subset of participants)

Supplementary figure 1 – Flowchart showing recruitment to CATNAP 1 and CATNAP 2, and the inclusion of participants in this analysis.